

# Improved conductivity-measurement of semiconductor epitaxial layers by means of the contactless microwave method

P. Boege\*, H. Schäfer\*, Xu Shanjia\*\*, Wu Xinzhang\*\*, S. Einfeldt\*,  
C.R. Becker\*, D. Hommel\* and R. Geick\*

\*Physikalisches Institut der Universität,  
Am Hubland, 97074 Würzburg, FRG

\*\*University of Science and Technology of China,  
Hefei, Anhui, 230026, People's Republic of China

## ABSTRACT

Measurements and calculations of the scattering-characteristics of stratified lossy dielectric blocks completely filling a waveguide cross section are presented. The method is used for contactless conductivity measurements of MBE-grown II-VI semiconductor layers.

## 1. INTRODUCTION

II-VI semiconductors show some inherent advantages for applications in infrared and millimeter wave techniques as well as optoelectronics due to a tunable band-gap from the infrared (CdHgTe) to the blue (ZnSe). The narrow gap materials are used as infrared detectors while the wide gap compounds are suitable for the realization of blue lasers. A common use suffers from problems at the growth of high quality epitaxial films due to incorporation of local defects as impurities, interstitials and vacancies. The strong tendency of self-compensation makes it often extremely difficult or even impossible to obtain good ohmic contacts. Nevertheless the exact knowledge of transport properties is essential for the optimization of MBE-growth conditions, thus it is necessary to go two ways simultaneously: Develop ohmic contacts for devices and determine the conductivity contactlessly for an improvement of MBE-growth conditions.

## 2. EXPERIMENTAL SETUP

A characterization method for the conductivity has been developed which uses the scattering of microwaves at the discontinuity between the empty waveguide and the part filled with the sample<sup>1</sup>. For this purpose, we use a microwave bridge with standard X-band rectangular waveguide technique and with facilities for continuous temperature variation between room temperature and 4.2 K and a magnetic field of 0.5 T for magnetoconductivity measurements. This method is the most appropriate one among a large variety of microwave methods because we have to cover a large range of conductivities from  $1(\Omega cm)^{-1}$  to about  $2000(\Omega cm)^{-1}$  for epitaxial layers and from  $10^{-3}(\Omega cm)^{-1}$  to  $10^{-1}(\Omega cm)^{-1}$  for substrates.

Up to now for these measurements the height of the semiconductor sample had to be chosen close to the height of the waveguide and special care to ensure good electric contact to the waveguide

walls had to be taken<sup>1</sup>. These precautions allowed a two-dimensional analysis of the scattering characteristics<sup>2</sup>. Nevertheless this sample preparation is inconvenient and time consuming: Often it is difficult to prepare the sample in the desired height with acceptable precision. Precise fixing is also difficult and the sample is soiled with contacting paste.

### 3. IMPROVEMENT OF SAMPLE MOUNTING STRUCTURE

In order to reach the situation of a simple and sufficiently short routine measurement with acceptable accuracy we propose in this paper a new sample mounting structure which is shown in Fig. 1.

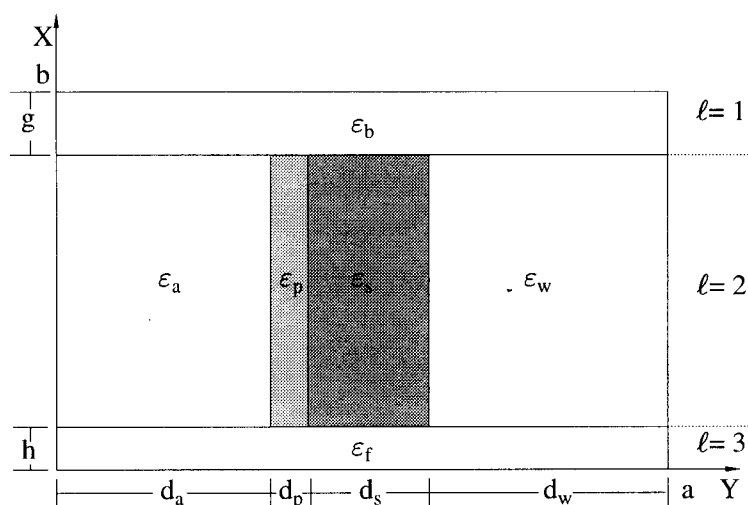


Fig.1 Cross section of the sample filled waveguide  
 $\epsilon_s, \epsilon_p$ : Dielectric constant of substrate and epitaxial layer  
 $\epsilon_a, \epsilon_w$ : Dielectric constant of sample mounting structure  
 $\epsilon_b, \epsilon_f$ : Dielectric constant of films for electric isolation of the sample

The sample height differs from the waveguide dimension. Two dielectric films having a dielectric constant  $\epsilon_f$  and  $\epsilon_b$  of about 2.0 are introduced as two transient regions in order to have a well defined microwave conducting between the sample and the walls of the waveguide. The other two dielectric blocks of polyurethane foam having the dielectric constant  $\epsilon_a$  and  $\epsilon_w$  of nearly 1.0 form the mounting structure to precisely fix the position of the sample in the waveguide so that the repeatability of the measurement is guaranteed.

The new mounting structure makes the measurement quicker and more reliable but this improvement has to be paid for with an extended and more elaborate mathematical analysis of the experimental data<sup>3</sup> compared to the simple situation of the partially filled waveguide with electric contacts mentioned before. We are dealing here with a complicated three dimensional scattering problem where especially the imaginary part of the complex dielectric constant of the layer covers a large range and where no perturbation theory can be used.

## 4. OUTLINE OF THE CALCULATION PROCEDURE

In this paper we will give a brief outline of the theory developed by Xu et al.<sup>3</sup>. The electromagnetic field boundary value problem is solved by combining multimode network theory with the rigorous mode matching procedure. The solution can be divided into two steps. First, the eigenvalue problem of the empty and of the filled waveguide are analysed in the transverse cross-section; secondly the scattering characteristics of the discontinuity in the longitudinal direction are calculated where the symmetry of the structure can be used to simplify the calculation procedure.

### 4.1 Eigenvalue problem of the empty waveguide

It is well known that the eigenfunctions of the empty waveguide are  $TE_{mn}$ - and  $TM_{mn}$ -modes and the field components can be written as:

$$E_x = \sum_{m,n} \left[ \overbrace{U'_{mn}(z) e'_{x,mn}(x,y)}^{TE_{mn}} + \overbrace{U''_{mn}(z) e''_{x,mn}(x,y)}^{TM_{mn}} \right] \quad (1)$$

$$E_y = \sum_{m,n} \left[ U'_{mn}(z) e'_{y,mn}(x,y) + U''_{mn}(z) e''_{y,mn}(x,y) \right] \quad (2)$$

$$E_z = \sum_{m,n} \left[ J''_{mn}(z) e''_{z,mn}(x,y) \right] \quad (3)$$

$$H_x = \sum_{m,n} \left[ J'_{mn}(z) h'_{x,mn}(x,y) + J''_{mn}(z) h''_{x,mn}(x,y) \right] \quad (4)$$

$$H_y = \sum_{m,n} \left[ J'_{mn}(z) h'_{y,mn}(x,y) + J''_{mn}(z) h''_{y,mn}(x,y) \right] \quad (5)$$

$$H_z = \sum_{m,n} \left[ U'_{mn}(z) h'_{z,mn}(x,y) \right] \quad (6)$$

where the auxiliary functions  $\vec{e}'_{mn}(x,y)$ ,  $\vec{h}'_{mn}(x,y)$ ,  $\vec{e}''_{mn}(x,y)$  and  $\vec{h}''_{mn}(x,y)$  describe the sin- and cos- dependence of the fields on x and y with wave vectors

$$q_x = \frac{m\pi}{a} ; q_y = \frac{n\pi}{b} \quad (7)$$

determined from boundary conditions at planes perpendicular to x and y, respectively.

### 4.2 Eigenvalue problem of the sample filled waveguide

It can be seen from Fig. 1 that the transverse cross section of the sample filled waveguide consists of three constituent parts ( $l = 1, 2, 3$ ). Each part supports two kinds of eigenmodes, one is the LSE and the other the LSM mode. The complete field distribution can be written as a superposition of LSE- and LSM-modes:

$$E_x = \sum_i U_i(z) \left[ \overbrace{\sum_m e'_{x,im}(x,y)}^{LSE} + \overbrace{\sum_n e''_{x,in}(x,y)}^{LSM} \right] \quad (8)$$

$$E_y = \sum_i U_i(z) \left[ \sum_n e''_{y,in}(x,y) \right] \quad (9)$$

$$E_z = \sum_i J_i(z) \left[ \sum_m e'_{z,im}(x,y) + \sum_n e''_{z,in}(x,y) \right] \quad (10)$$

$$H_x = \sum_i J_i(z) \left[ \sum_m h'_{x,im}(x,y) + \sum_n h''_{x,in}(x,y) \right] \quad (11)$$

$$H_y = \sum_i J_i(z) \left[ \sum_m h'_{y,im}(x,y) \right] \quad (12)$$

$$H_z = \sum_i U_i(z) \left[ \sum_m h'_{z,im}(x,y) + \sum_n h''_{z,in}(x,y) \right] \quad (13)$$

The auxiliary functions  $\vec{e}'_{im}(x,y)$ ,  $\vec{h}'_{im}(x,y)$ ,  $\vec{e}''_{in}(x,y)$  and  $\vec{h}''_{in}(x,y)$  (for details see Reference 3, Table 2) are defined separately in each subregion  $l$ ,  $i$  denotes the mode number in the sample filled waveguide.

The  $y$ -dependence of the auxiliary functions (Ref.3, Eqs.22,23) is determined using the boundary conditions at planes perpendicular to  $y$  separately for each part  $l$  by extending each part infinitely wide in  $x$ -direction. Thus the modefunctions and the corresponding wave number components  $k'_{ym,l}$  and  $k''_{yn,l}$  are determined.

All  $k_{zi}$  for the complete structure are calculated by transverse resonance method using boundary conditions at planes perpendicular to  $x$  together with mode matching between the parts in  $x$ -direction (Ref.3, Eqs.42-49). Thus all partial solutions for each part  $l$  are recombined to the complete sample structure thereby deriving the  $x$ -dependence of the auxiliary functions mentioned before (Ref.3, Eqs.74,75) and the corresponding wave number components  $k'_{xim,l}$  and  $k''_{xin,l}$ . These components of the wave vectors fulfill the usual wave equation ( $k_0 = \frac{\omega}{c}$ ) thus defining  $k'_{xim,l}$  and  $k''_{xin,l}$ .

$$k_0^2 \varepsilon_l(y) = k_{xim,l}^{\prime 2} + k_{ym,l}^{\prime 2} + k_{zi}^2 \quad (14)$$

$$k_0^2 \varepsilon_l(y) = k_{xin,l}^{\prime \prime 2} + k_{yn,l}^{\prime \prime 2} + k_{zi}^2 \quad (15)$$

Up to now the functions  $U_i(z)$  and  $J_i(z)$  are still unknown, only the corresponding  $k_{zi}$  are determined.  $U_i(z)$  and  $J_i(z)$  have to be calculated by mode matching at the sample discontinuity in longitudinal direction (Ref.3, Eqs.89,90). Fig.2 shows the sample structure looking from the top waveguide wall to the bottom.

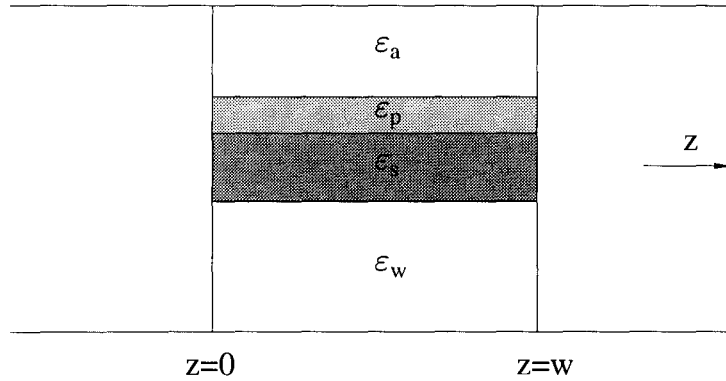


Fig.2 Sample structure in longitudinal direction

For the  $z$ -dependence the following Ansatz can be made for the transverse field components  $E_x$  and  $E_y$  of  $\vec{E}$  taking into account that the incident wave is only a  $TE_{10}$ -mode in our experiment.

$z < 0 :$

$$\vec{E}_t = \vec{e}'_{10}(x, y) H'_{10} e^{-j q'_{10} z} + \sum_{m, n} \left[ \vec{e}'_{mn}(x, y) R'_{mn} e^{j q'_{mn} z} + \vec{e}''_{mn}(x, y) R''_{mn} e^{j q''_{mn} z} \right] \quad (16)$$

$0 \leq z \leq w :$

$$\vec{E}_t = \sum_i \vec{e}_i(x, y) \left[ \underbrace{U_{si} \cos(k_{zi}(z - \frac{w}{2})) + U_{ai} \sin(k_{zi}(z - \frac{w}{2}))}_{U_i(z)} \right] \quad (17)$$

$z > w :$

$$\vec{E}_t = \sum_{m, n} \left[ \vec{e}'_{mn}(x, y) \underbrace{T'_{mn} e^{-j q'_{mn} z}}_{U'_{mn}(z)} + \vec{e}''_{mn}(x, y) \underbrace{T''_{mn} e^{-j q''_{mn} z}}_{U''_{mn}(z)} \right] \quad (18)$$

$$\approx \vec{e}'_{10}(x, y) T'_{10} e^{-j q'_{10} z} \quad \text{for large } z \gg w$$

Similar equations hold for the transverse field components  $H_x$  and  $H_y$  of  $\vec{H}$ . When the coefficients  $R'_{mn}$ ,  $R''_{mn}$ ,  $T'_{mn}$  and  $T''_{mn}$  are determined by mode matching at  $z = 0$  and  $z = w$  the complex transmission coefficient  $S_{21}$  is given by  $S_{21} = T'_{10} e^{j q'_{10} w} / H'_{10}$ . The calculation is simplified strongly by using the symmetry of the structure at  $z = \frac{w}{2}$ .<sup>2</sup>

## 5. THEORETICAL AND EXPERIMENTAL RESULTS

The geometry, the complex dielectric constants of the sample and the sample mounting structure have an important influence on the transmitted and reflected microwave power. Because in our experiment the transmission of the the incident  $TE_{10}$ -mode is the measurable quantity, we show numerical and experimental results for the complex transmission coefficient  $S_{21} = |S_{21}|e^{j\varphi_{21}}$  in dependence on the conductivity  $\sigma$  of the epitaxial layer, the thickness  $g$  of the gap between sample and top waveguide wall and the length  $w$  of the sample. All other parameters as conductivity of the substrate, thickness of substrate and epitaxial layer, dimensions and dielectric constants of the sample mounting structure and the frequency of the microwave are kept constant. Usual values in our experiments are (see Fig.1):

Conductivity of substrate:	$\sigma_s = 10^{-8}(\Omega cm)^{-1}$	or	$\sigma_s = 2.5 \cdot 10^{-3}(\Omega cm)^{-1}$
Thickness of substrate:	$d_s = 0.5mm$	or	$d_s = 0.8mm$
Thickness of epitaxial layer:	$d_p = 1.0\mu m$		
Thickness of polyester foil:	$h = 0.1mm$		
Thickness of polyurethane foam:	$d_w = 10.0mm$		
Frequency:	$f = 8.89GHz$		

Fig. 3 shows numerical results for the dependence of phase shift  $\varphi_{21}$  and damping  $|S_{21}|$  on the conductivity of the epitaxial layer for three different gaps  $g$  (see Fig.1) between sample and top waveguide wall with fixed sample length.

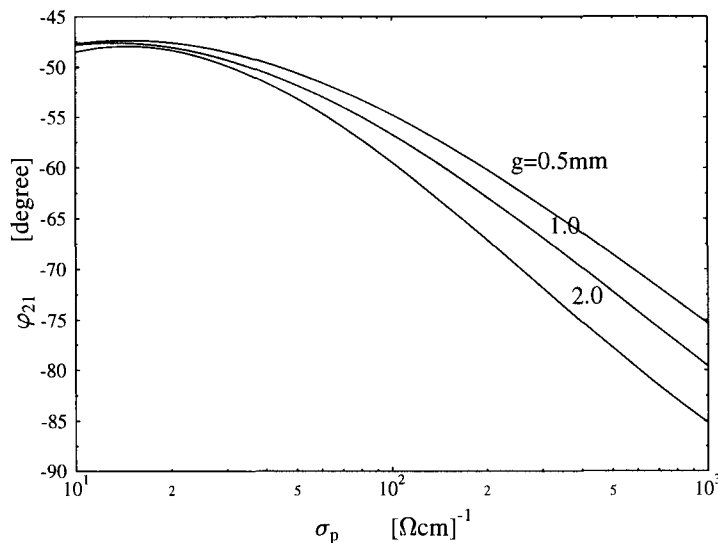


Fig. 3.1 Variation of  $\varphi_{21}$  with the conductivity of the epitaxial layer

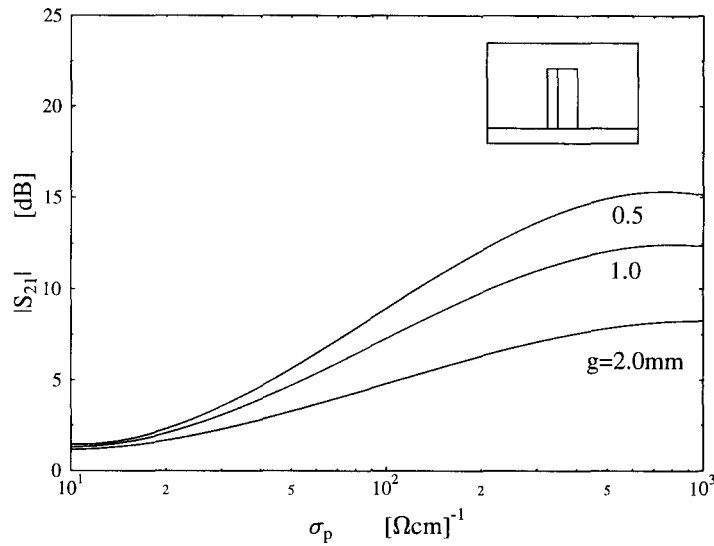


Fig. 3.2 Variation of  $|S_{21}|$  with the conductivity of the epitaxial layer

While the phase shift shows a steep dependence on the conductivity in the range from  $30(\Omega cm)^{-1}$  to  $1000(\Omega cm)^{-1}$  even for large gaps, the damping is only sensitive on the conductivity in the range from  $30(\Omega cm)^{-1}$  to  $500(\Omega cm)^{-1}$ . The sensitivity decreases strongly with increasing gap.

In order to verify the dependence of the transmission coefficient on the gap between sample and waveguide, a sample of CdHgTe with a conductivity of  $550(\Omega cm)^{-1}$  has been reduced step by step in height by cutting. This influence is the most important difference compared to the old sample preparation<sup>1,2</sup>. Fig. 4 shows a comparison of theoretical and experimental results for the dependence of the transmission coefficient on the gap.

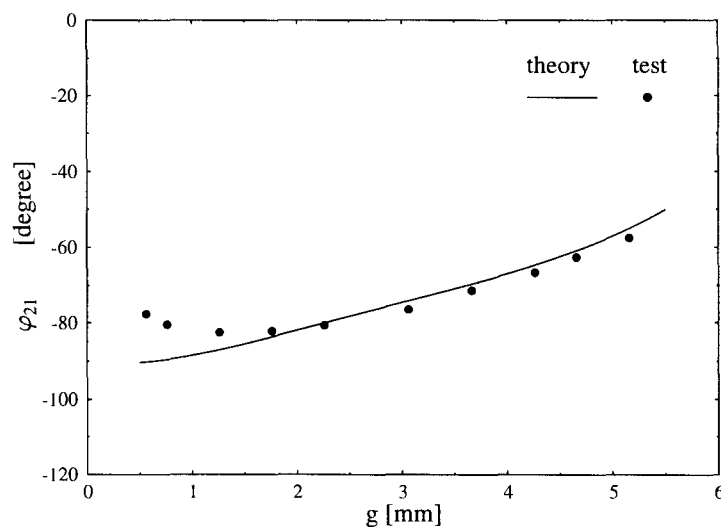


Fig. 4.1 Variation of  $\varphi_{21}$  with the gap of the sample

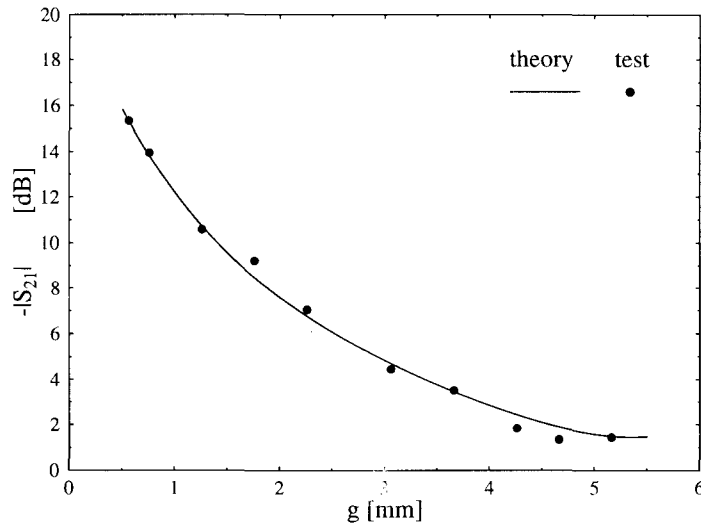


Fig. 4.2 Variation of  $|S_{21}|$  with the gap of the sample

The damping of the transmitted power decreases strongly with decreasing sample height, mainly due to less lossy material present in the sample structure. The phase shift changes from about  $90^\circ$  to  $50^\circ$  when the sample height is reduced by 5 mm. Thus for a precise determination of the layer conductivity the gap has to be determined carefully in order to avoid misinterpretation of the measured quantities.

The same holds for the influence of the sample length  $w$  (see Fig.2) on the transmission coefficient which is shown in Fig. 5 for different values of the gap  $g$ .

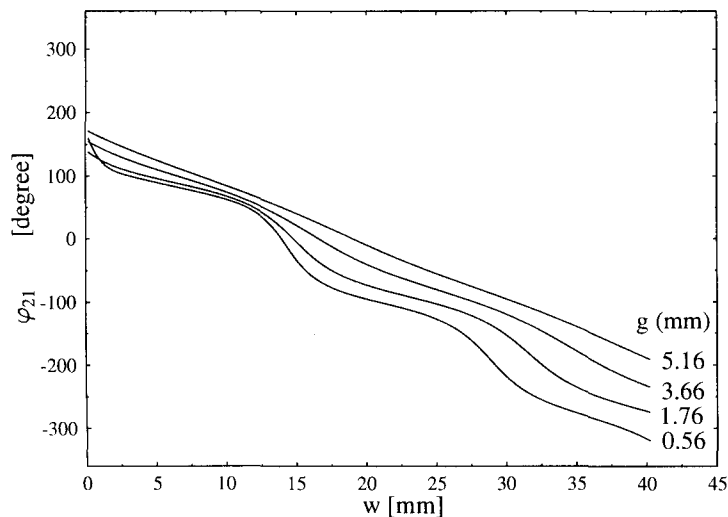


Fig. 5.1 Variation of  $\varphi_{21}$  with the length of the sample



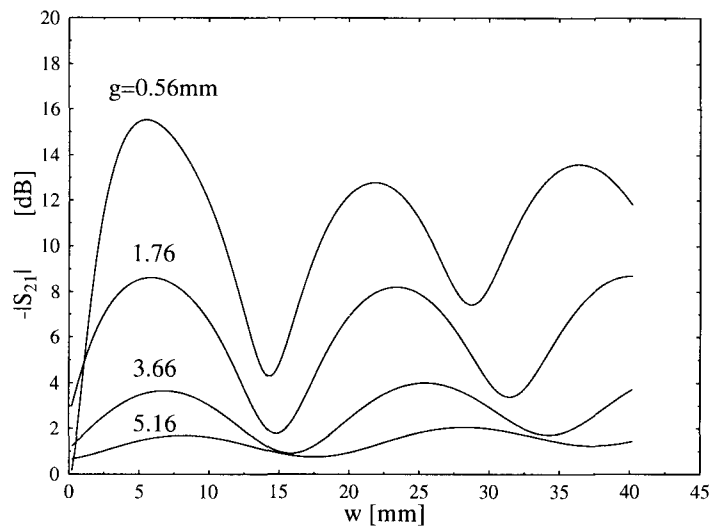


Fig. 5.2 Variation of  $|S_{21}|$  with the length of the sample

Especially for small gaps  $g$  the damping shows a pronounced periodic resonant-like behaviour in dependence on the sample length which is also slightly visible in the phase shift. In order to reach maximum accuracy the sample length should be chosen close to a region where the dependence of the transmission coefficient on the sample length is flat, i.e. close to a maximum in Fig. 5.2 .

## 6. CONCLUSIONS

The use of the new sample mounting structure in a microwave bridge in combination with the calculations presented here allows a contactless temperature dependent measurement of the DC-transport attributes of epitaxial layers in the as-grown state without time consuming preparation and without soiling of the sample. Nearly the whole range of conductivities of the layers is covered by this technique. Further improvements will be concerned with the introduction of the dielectric constant as a tensor in order to measure the Hall-effect at low magnetic fields available here and with an increase of the sensitivity at low conductivities by focusing the electric field on the epitaxial layer with dielectric blocks in the waveguide.

## 7. ACKNOWLEDGEMENT

Support of the National Natural Foundation of China and the Deutsche Forschungsgemeinschaft is gratefully acknowledged.

## 8. REFERENCES

1. P.Greiner, L.Polignone, C.R.Becker and R.Geick, "Contactless measurement of the conductivity of II-VI epitaxial layers by means of the partially filled waveguide method", *Appl.Phys.* A55, pp. 279-288, 1992
2. Xu Shanjia, Wu Xinzhang, P.Greiner, C.R.Becker and R.Geick, "Microwave transmission and reflection of stratified lossy dielectric segments partially filling waveguide", *Int'l J. of Infrared and Millimeter Waves* 13, pp. 569-587, 1992
3. Xu Shanjia, Wu Xinzhang, P.Boege, H.Schäfer, C.R.Becker and R.Geick, "Scattering characteristics of 3-D discontinuity consisting of semiconductor sample filled in waveguide with gaps", *Int'l J. of Infrared and Millimeter Waves* 14, pp.2155-2190, 1993